

EMFlow: Data Imputation in Latent Space via EM and Deep Flow Models

Qi Ma Sujit K. Ghosh

Department of Statistics, North Carolina State University, Raleigh

{qma4, sujit.ghosh}@ncsu.edu

Abstract

High dimensional incomplete data can be found in a wide range of systems. Due to the fact that most of the data mining techniques and machine learning algorithms require complete observations, data imputation is vital for down-stream analysis. In this work, we introduce an imputation approach, called EMFlow, that performs imputation in an latent space via an online version of Expectation-Maximization (EM) algorithm and connects the latent space and the data space via the normalizing flow (NF). The inference of EMFlow is iterative, involving updating the parameters of online EM and NF alternatively. Extensive experimental results on multivariate and image datasets show that the proposed EMFlow has superior performance to competing methods in terms of both imputation quality and convergence speed.

1. Introduction

Missingness is ubiquitous for real-world datasets and is a major issue of data quality as it adversely impact the validity of down-stream analysis. Most machine learning algorithms and statistical tools are not robust to the bias introduced by missing data, which could results in inferior accuracy or loss of power [20, 33, 34].

State of art imputation methods exploits the development of machine learning techniques. Early works in this field perform imputation in a supervised manner where a complete training set is needed to learning the correlation between missing and observed entries [e.g. 2, 14, 30, 39, 40]. However, it's common that a large collection of fully observed data is hard to acquire, which makes those data-greedy supervised algorithms less effective. On the other hand, early attempts in unsupervised imputation methods, such as the collaborative filtering [32], usually learn the correlation across dimensions by embedding the data into a lower dimensional latent space linearly [e.g. 1, 23]. But the representation power of those linear models are limited when dealing with complex datasets.

More recently, several imputation methods based on

deep generative models have been proposed, providing much more accurate estimates of missing values especially for high-dimensional image datasets. In this work, we introduce *EMFlow* that integrates the normalizing flow (NF) [11, 12, 17, 29] with an online version of Expectation-Maximization (EM) algorithm [6]. The proposed framework is motivated by the strength and weakness of EM. As a class of iterative algorithm designed for latent variable models, EM can be applied to data imputation in an interoperable way [23]. Additionally, the learning of EM is usually numerically stable and its convergence property has been studied extensively [e.g. 25, 27, 37, 42]. However, the E-step and M-step are only traceable with simple underlying distributions including multivariate Gaussian or Student's t distributions as well as their mixtures [e.g. 10, 38]. On the other hand, NF is capable of latent representation and efficient data sampling, which makes it a convenient bridge between the data space and the latent space. Therefore, we let EM perform imputation in the latent space where simple inter-feature dependency is assumed (i.e. the underlying distribution is multivariate Gaussian). Meanwhile, NF is used to recover the mapping between the complex inter-feature dependency in the data space and the one in the latent space learned by EM.

The inference of EMFlow adopts an iterative learning strategy that has been widely used model-based multiple imputation methods where the initial naive imputation is refined step by step until convergence [e.g. 5, 15, 35]. Specifically, three steps are performed alternatively: update the density estimation of complete data including the observed and current imputed values; update the base distribution (i.e. μ and Σ) in the latent space by EM; and update the imputation in the data space. Note that the first update corresponds to optimizing the complete data likelihood as well as the reconstruction error computed on the observed entries. We also derive an online version of EM such that it only consumes a batch of data at a time for parameter update and thus can work with deep generative models smoothly. We will show that such learning schema has simple implementation and leads to fast convergence.

The main contributions of this work are as follows:

- 1) an imputation framework combining an online version of Expectation-Maximization (EM) algorithm and the normalizing flow;
- 2) an iterative learning schema that alternatively updates the inter-feature dependency in the latent space (i.e. the base distribution) and density estimation in the data space;
- 3) a derivation of online EM in the context of missing data imputation; and
- 4) extensive experiments on multiple image and tabular datasets to demonstrate the imputation quality and convergence speed of the proposed framework.

2. Related work

Recently, the applications of deep generative models like Generative Adversarial Networks (GAN) [28] have been extended to the field of missing data imputation under the assumption of Missing at Random (MAR) or Missing Completely at Random (MCAR). The authors of GAIN [41] design a compete data generator that performs imputation, and a discriminator to differentiate imputed and observed components with the help of a *hint* mechanism. MisGAN [22] introduces another pair of generator-discriminator that aims to learn the distribution of missing mask. However, training GAN-based models is a notoriously challenging for its excessively complex structure and non-convex objectives. For example, MisGAN optimizes three objectives jointly involving six neural networks. Furthermore, GAN-based models do not obtain explicit density estimation that could be critical for down-stream analysis.

Some imputation techniques based on Variational Autoencoders (VAE) [18] are also developed. For example, MIWAE [26] leverages the importance-weighted autoencoder [4] and optimizes a lower bound of the likelihood of observed data. But the zero imputation adopted by it can be problematic since observed entries can also be zero. It also needs quite large computational power to make the bound to be tight. EDDI [24] avoids zero imputation by introducing a permutation invariant encoder. Imputation under Missing not at Random (MNAR) has also been explored by explicitly modeling the missing mechanism [8, 16]. However, all VAE-based approaches only permit approximate density estimation no matter how expressive the inference model is.

Our proposed framework builds on the work of MCFlow [31] that utilizes NF to learn exact density estimation on incomplete data via an iterative learning schema. The core component of MCFlow is a feed forward network that operates in the latent space and attempts to find the likeliest embedding vector in a supervised manner. Although MCFlow achieves impressive performance compared to other state of art methods, it remains ambiguous that how the feed forward network exploits the correlation in the latent space.

We also find that the inference of MCFlow often has slow convergence speed and can be unstable.

3. Approach

3.1. Problem Definition

We define the complete dataset \mathbf{X} as a collection of vectors $\{\mathbf{x}_1, \dots, \mathbf{x}_n\}$ that are i.i.d. samples drawn from $p_X(\cdot; \theta)$ in a p -dimensional data space. The missing pattern of \mathbf{x}_i is described by a binary mask $\mathbf{m}_i \in \{0, 1\}^p$ such that \mathbf{x}_{ij} is missing if $\mathbf{m}_{ij} = 1$, and \mathbf{x}_{ij} is observed if $\mathbf{m}_{ij} = 0$.

Let \mathbf{x}^o and \mathbf{x}^m be the observed and missing parts of \mathbf{x} , and $p_M(\mathbf{m}|\mathbf{x}) = p_M(\mathbf{m}|\mathbf{x}^o, \mathbf{x}^m)$ be the conditional distribution of the mask. Based on dependency between \mathbf{m} and $(\mathbf{x}^o, \mathbf{x}^m)$, the missing mechanism can be classified into three classes [23]:

- MCAR: $p_M(\mathbf{m}|\mathbf{x}^o, \mathbf{x}^m) = p_M(\mathbf{m})$
- MAR: $p_M(\mathbf{m}|\mathbf{x}^o, \mathbf{x}^m) = p_M(\mathbf{m}|\mathbf{x}^o)$
- MNAR: The probability of missing depends on both \mathbf{x}^o and \mathbf{x}^m .

Throughout this paper, we only focus on MCAR or MAR where the missing mechanism can be safely ignored. Our goal is to minimize the reconstruction error between the complete data \mathbf{X} and its imputed version $\hat{\mathbf{X}}$ by optimizing the observed data log-likelihood:

$$L^{obs}(\theta) = \sum_{i=1}^n \log \int p_X(\mathbf{x}_i^o, \mathbf{x}_i^m; \theta) d\mathbf{x}_i^m \quad (1)$$

We also expect to obtain the density estimation \hat{p}_X as a by-product of the imputation.

3.2. Normalizing Flows

The basic idea behind normalizing flow is to find a transformation (of X) that would be able to represent a complex density function as a function of simpler ones, such as a multivariate Gaussian random variable (to be denoted by Z). The quest for the transformation $Z = f(X) \sim \bar{N}_p(0, I)$ can be challenging, but in theory such a transformation does exist. Brockwell [3] showed the existence of such a transformation which converts any p -dimensional random variable X to p independent uniform random variables $U_j = g_j(X) \sim U(0, 1)$ for $j = 1, \dots, p$, which are known are universal residuals. Thus, choosing $Z_j = f_j(X) \equiv \Phi^{-1}(g_j(X)) \sim N(0, 1)$, where $\Phi(\cdot)$ denotes the cumulative distribution function of a standard normal distribution, we can show the existence of $Z = f(X)$, where $f(x) = (f_1(x), \dots, f_p(x))$ that enables to transform X to Z . However, finding such nonlinear transform based on observed data is challenging and so we use sequence of simpler transforms in the spirit of universal residuals, for simplicity and computational efficiency.

To make it possible to optimize Eq. (1), $p_X(\mathbf{x}; \theta)$ needs to be specified in a parametric way that should be expressive enough, as the density is potentially complex and high-dimensional. To this end, we use NF to model $p_X(\mathbf{x}; \theta)$ as an invertible transformation f_ψ of a base transformation $p_Z(z; \phi)$ in the latent space \mathcal{Z} . Under the change of variables theorem, the complete data log-density is specified as

$$p_X(\mathbf{x}; \theta) = p_Z(f_\psi^{-1}(\mathbf{x}); \phi) \left| \det \left(\frac{\partial f_\psi^{-1}(\mathbf{x})}{\partial \mathbf{x}^T} \right) \right| \quad (2)$$

where $\theta = (\psi, \phi)$.

f_ψ is usually composed by a sequence of relatively simple transformations to approximate arbitrarily complex distributions with high representation power. In this work, we choose RealNVP [12] based on affine coupling transformations as the flow model¹. Recently, Teshima et al. [36] has shown that normalizing flow models constructed on affine coupling layers can be universal distributional approximators.

Data imputation relies on the inter-feature dependency that is usually intractable and hard to capture in the data space \mathcal{X} with the presence of missing entries. Therefore, we make the following two assumptions.

Assumption 1: The inter-feature dependency in the latent space \mathcal{Z} is simple and can be characterized by a multivariate Gaussian distribution, that is:

$$p_Z(\mathbf{z}; \phi) = \mathcal{N}(\mathbf{z}; \mu, \Sigma) \quad (3)$$

where $\phi = (\mu, \Sigma)$.

Note that the base distribution is usually a standard Gaussian distribution in the literature for simplicity. However, the covariance Σ is essential in our work to represent the inter-feature dependency.

Assumption 2: Given that the transformations involved in NF are feature-wise [e.g. 11, 12], we expect NF to learn the mapping between the complex inter-feature dependency in the data space \mathcal{X} and the simple one in the latent space \mathcal{Z} .

3.3. Online EM

EM is a class of general iterative algorithms for latent variable models including missing data imputation[23]. In EMFlow, it would work in the latent space \mathcal{Z} where the underlying distribution is $\mathcal{N}(\mathbf{z}; \mu, \Sigma)$. Given the embedding vectors $\{\mathbf{z}_1, \dots, \mathbf{z}_n\}$ where $\mathbf{z}_i = f_\psi^{-1}(\mathbf{x}_i)$, and the corresponding missing mask $\{\mathbf{m}_1, \dots, \mathbf{m}_n\}$, EM aims to estimate (μ, Σ) in an iterative way:

¹The details of RealNVP are provided in the supplementary section.

$$\begin{aligned} \hat{\mu}^{(t)} &= g_\mu(\hat{\mu}^{(t-1)}, \hat{\Sigma}^{(t)}; \{\mathbf{z}_i, \mathbf{m}_i\}_{i=1}^n) \\ \hat{\Sigma}^{(t)} &= g_\Sigma(\hat{\mu}^{(t-1)}, \hat{\Sigma}^{(t)}; \{\mathbf{z}_i, \mathbf{m}_i\}_{i=1}^n) \end{aligned} \quad (4)$$

where $(\hat{\mu}^{(t)}, \hat{\Sigma}^{(t)})$ are the estimates at the t^{th} iteration, and $\{g_\mu(\cdot), g_\Sigma(\cdot)\}$ denote the mappings between two consecutive iterations².

Given the estimates $(\hat{\mu}, \hat{\Sigma})$, the conditional mean is used for imputation:

$$\begin{aligned} \hat{\mathbf{z}}_i^m &= E(\mathbf{z}_i^m | \mathbf{z}_i^o; \hat{\mu}, \hat{\Sigma}) \\ &= \hat{\mu}_{\mathbf{m}_i} + \hat{\Sigma}_{\mathbf{m}_i \mathbf{o}_i} \left(\hat{\Sigma}_{\mathbf{o}_i \mathbf{o}_i} \right)^{-1} (\mathbf{z}_i^o - \hat{\mu}_{\mathbf{o}_i}) \end{aligned} \quad (5)$$

where \mathbf{z}_i^m and \mathbf{z}_i^o are the missing and observed parts of \mathbf{z}_i , \mathbf{o}_i is the observed mask (i.e. the complement of \mathbf{m}_i), and the subscripts of $(\hat{\mu}, \hat{\Sigma})$ denotes the slicing indexes.

When processing datasets of large volume, EM becomes impractical because it needs to read the whole data into the memory for each iteration. Following the framework introduced by Cappé and Moulines [6], we drive an online version of EM algorithm in the context of data imputation. Let $B \subset \{1, \dots, n\}$ denote a mini-batch of sample indexes, the online EM first obtain *local* estimates:

$$\begin{aligned} \hat{\mu}_{batch} &= g_\mu(\hat{\mu}^{(t)}, \hat{\Sigma}^{(t)}; \{\mathbf{z}_i, \mathbf{m}_i\}_{i \in B}) \\ \hat{\Sigma}_{batch} &= g_\Sigma(\hat{\mu}^{(t)}, \hat{\Sigma}^{(t)}; \{\mathbf{z}_i, \mathbf{m}_i\}_{i \in B}) \end{aligned} \quad (6)$$

The *global* estimates are then computed in the fashion of moving average:

$$\begin{aligned} \hat{\mu}^{(t)} &= \rho_t \hat{\mu}_{batch} + (1 - \rho_t) \hat{\mu}^{(t-1)} \\ \hat{\Sigma}^{(t)} &= \rho_t \hat{\Sigma}_{batch} + (1 - \rho_t) \hat{\Sigma}^{(t-1)} \end{aligned} \quad (7)$$

where (ρ_0, ρ_1, \dots) are a sequence of step sizes satisfying

$$0 < \rho_t < 1, \sum_{i=1}^{\infty} \rho_i = \infty \text{ and } \sum_{i=1}^{\infty} \rho_i^2 < \infty \quad (8)$$

In this work, we use a step size schedule defined by

$$\rho_t = C t^{-\gamma} \quad (9)$$

where C is a positive constant and $\gamma \in (0.5, 1]$.

3.4. Architecture and Inference

EMFlow is a composite framework that combines NF and online EM. As illustrated in Fig 1, NF is the bidirectional tunnel between the data space and the latent space, aiming to learn the complete data density p_X . In the latent space, the online EM estimates the inter-feature dependency

²See Appendix for the details of g_μ and g_Σ .

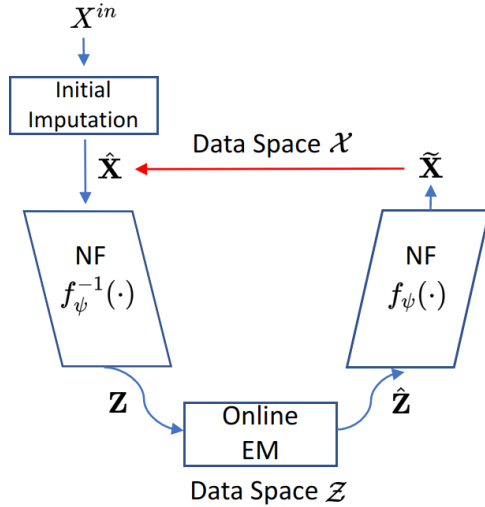


Figure 1. EMFlow architecture.

of the embedding vectors and performs imputation. To address the issue that NF needs complete data vectors for computation, the incomplete data \mathbf{X}^{in} are imputed naively (e.g. median imputation for tabular datasets) at the very beginning to get the *initial* current imputed data $\hat{\mathbf{X}}$. Afterwards, the objective in Eq. (1) is optimized in an iterative schema, where each iteration consists of a training phase and a re-imputation phase.

Training Phase At this phase, the current imputed data $\hat{\mathbf{X}}$ stay fixed, while the parameter estimates of NF (i.e. $\hat{\psi}$) and base distribution (i.e. $\hat{\mu}$ and $\hat{\Sigma}$) are updated in different ways.

First of all, given the current estimated base distribution $\mathcal{N}(\mathbf{z}; \hat{\mu}, \hat{\Sigma})$, the flow model f_{ψ} are learned by optimizing the negative log-likelihood of a batch of the current imputed data $\hat{\mathbf{X}}_B$:

$$L_1(\psi) = -\frac{1}{n} \sum_{i \in B} p_X(\hat{\mathbf{x}}_i; \psi, \hat{\mu}, \hat{\Sigma}) \quad (10)$$

The computation of L_1 requires exact likelihood evaluation that is equipped by NF. Once the flow model parameters get updated, we obtain the embedding vectors in the latent space:

$$\mathbf{z}_i = f_{\psi}^{-1}(\hat{\mathbf{x}}_i), \quad i \in B \quad (11)$$

Although the embedding vectors are complete, they are treated as incomplete using the missing masks in the data space $\{\mathbf{m}_i\}_{i \in B}$, given that the invertible mapping parameterized by f_{ψ} is feature-wise. Therefore, the online EM impute the missing parts of the embedding vectors with the current global estimates $(\hat{\mu}, \hat{\Sigma})$:

$$\hat{\mathbf{z}}_i^m = E(\mathbf{z}_i^m | \mathbf{z}_i^o; \hat{\mu}, \hat{\Sigma}), \quad i \in B \quad (12)$$

which results in new embedding vectors $\{\hat{\mathbf{z}}_i\}_{i \in B}$ where $\hat{\mathbf{z}}_i$ consists of the observed part \mathbf{z}_i^o and the imputed part $\hat{\mathbf{z}}_i^m$. After the imputation, the global estimates $(\hat{\mu}, \hat{\Sigma})$ are updated following Eq. (6) and (7).

Since the base distribution has been changed, it's necessary to update the flow model f_{ψ} again by optimizing a composite loss:

$$L_2(\psi) = -\frac{1}{|B|} \sum_{i \in B} \left[p_X(\tilde{\mathbf{x}}_i; \psi, \hat{\mu}, \hat{\Sigma}) - \alpha L_{\text{rec}}(\tilde{\mathbf{x}}_i, \hat{\mathbf{x}}_i, \mathbf{m}_i) \right] \quad (13)$$

where $|B|$ denotes the batch size, $\tilde{\mathbf{x}}_i = f_{\psi}(\hat{\mathbf{z}}_i)$, and $L_{\text{rec}}(\tilde{\mathbf{x}}_i, \hat{\mathbf{x}}_i, \mathbf{m}_i)$ is the reconstruction error only for non-missing values:

$$L_{\text{rec}}(\tilde{\mathbf{x}}_i, \hat{\mathbf{x}}_i, \mathbf{m}_i) = \sum_{j=1}^p (1 - \mathbf{m}_{ij})(\tilde{\mathbf{x}}_{ij} - \hat{\mathbf{x}}_{ij})^2 \quad (14)$$

In this composite loss, the first term forces the reconstructed data vectors $\{\tilde{\mathbf{x}}_i\}_{i \in B}$ to have high likelihood in the data space, while the second term encourages $\{\tilde{\mathbf{x}}_i\}_{i \in B}$ to match the observed parts of the incomplete training data. And since $\{\tilde{\mathbf{x}}_i\}_{i \in B}$ are transformed from $\{\hat{\mathbf{z}}_i\}_{i \in B}$ via f_{ψ} , both terms are conditioned on the inter-feature dependency learned by EM. A pseudocode for this training phase is presented in Algorithm 1.

Algorithm 1 Training Phase

- 1: **Input:** Current imputation: $\hat{\mathbf{X}} = (\hat{\mathbf{x}}_1, \dots, \hat{\mathbf{x}}_n)^T$, missing masks $\mathbf{M} = (\mathbf{m}_1, \dots, \mathbf{m}_n)^T$, initial estimates of the base distribution $(\hat{\mu}^{(0)}, \hat{\Sigma}^{(0)})$, online EM step size sequence: $\rho_1, \rho_2, \dots, \rho_t, \dots$
- 2: **for** $t = 1$ to T_{epoch} **do**
- 3: Get a mini-batch $\hat{\mathbf{X}}_B = \{\hat{\mathbf{x}}_i\}_{i \in B}$
- 4: **# update the flow model**
- 5: Compute L_1 in Eq. (10)
- 6: Update ψ via gradient descent
- 7: **# update the base distribution**
- 8: $\mathbf{z}_i = f_{\psi}^{-1}(\hat{\mathbf{x}}_i), \quad i \in B$
- 9: Impute in the latent space with $(\hat{\mu}^{(t-1)}, \hat{\Sigma}^{(t-1)})$ to get $\{\hat{\mathbf{z}}_i\}_{i \in B}$ via Eq. (12)
- 10: Obtain updated $(\hat{\mu}^{(t)}, \hat{\Sigma}^{(t)})$ via Eq. (6) and (7)
- 11: **# update the flow model again**
- 12: $\tilde{\mathbf{x}}_i = f_{\psi}(\hat{\mathbf{z}}_i), \quad i \in B$
- 13: Compute L_2 Eq. 13
- 14: Update ψ via gradient descent

Re-Imputation Phase After the training phase, the re-imputation phase is executed to update the current imputation. This procedure is similar to that in the training phase, except that all model parameters are kept fixed. As shown by the last line of Algorithm 2, the missing parts of the current imputation are replaced with those of the reconstructed data vectors.

Algorithm 2 Re-imputation Phase

- 1: **Input:** Current imputation: $\widehat{\mathbf{X}} = (\widehat{\mathbf{x}}_1, \dots, \widehat{\mathbf{x}}_n)^T$, missing masks $\mathbf{M} = (\mathbf{m}_1, \dots, \mathbf{m}_n)^T$, estimates of the base distribution $(\widehat{\mu}, \widehat{\Sigma})$ from the previous training phase
- 2: **for** $i = 1$ to n **do**
- 3: $\mathbf{z}_i = f_{\psi}^{-1}(\widehat{\mathbf{x}}_i)$
- 4: Impute in the latent space with $(\widehat{\mu}, \widehat{\Sigma})$ to get $\widehat{\mathbf{z}}_i$ via Eq. (12)
- 5: $\widetilde{\mathbf{x}}_i = f_{\psi}(\widehat{\mathbf{z}}_i)$
- 6: **# update current imputation**
- 7: $\widehat{\mathbf{x}}_i = \widehat{\mathbf{x}}_i \odot \mathbf{o}_i + \widetilde{\mathbf{x}}_i \odot \mathbf{m}_i$

3.5. Implementation Details

Model Initialization Each inference iteration consists of a training phase and a re-imputation phase. And since the latter phase updates the current imputation, the parameters of the flow model f_{ψ} are reinitialized after each iteration to learn the new data density faster.

The base distribution estimate $\mathcal{N}(\mathbf{z}; \widehat{\mu}, \widehat{\Sigma})$ is initialized at the very beginning when the online EM encounters the first batch of embedding vectors \mathbf{Z}_B . Specifically $\widehat{\mu}$ and $\widehat{\Sigma}$ are initialized to be the sample mean and sample covariance of \mathbf{Z}_B . By default, the base distribution is reinitialized along with the flow model after each iteration.

Stabilization of Online EM Online EM can be unstable in some cases where the estimate of covariance $\widehat{\Sigma}$ becomes ill-conditioned during the inference. Such instability can be traced back to two primary sources: (i) the initial naive imputation has really bad quality and the inter-feature dependency is distorted significantly; (ii) the batch size is close to or less than the number of features, which makes it hard to estimate the covariance directly [e.g. 7, 13].

Fortunately, those two issues can be solved easily. To reduce the impact of the initial naive imputation and make the covariance estimation more robust, we enlarge the diagonal entries of the original covariance estimate from Eq. (7) proportionally:

$$\widehat{\Sigma}^{Rob} = \widehat{\Sigma} + \beta \cdot \text{Diag}(\widehat{\Sigma}) \quad (15)$$

where $\text{Diag}(\widehat{\Sigma})$ is a diagonal matrix with the same diagonal entries as $\widehat{\Sigma}$, and β a positive hyperparameter. In practice, β

would be decreased gradually to 0 during the first a few iterations of the inference as the quality of current imputation gets better and better.

To address the second issue, the training phase in Algorithm 1 can be modified to make the online EM see more data points. When updating the base distribution, the current batch of embedding vectors can be concatenated with previous ones to form a *super*-batch with a maximum size S_{super} . If the maximum size is exceeded, the most previous embedding vectors would be excluded. And since the previous batches are already imputed, the super-batch brings nearly no additional computational overhead.

4. Experiments

In this section, we evaluate the performance of EMFlow on multivariate and datasets in terms of the imputation quality and the speed of model training. Its performance is compared to that of MCFlow, the most related competitor that has been shown to be superior to other state of art methods [31].

To make the comparison more objective, both models use the same normalizing flow with six affine coupling layers. We also follow the authors' suggestion for the the hyperparameter selection of MCFlow throughout this section.

4.1. Multivariate Datasets

Ten multivariate datasets from the UCI repository [9] are used for evaluation. For all of them, each feature is scaled to fit inside the interval $[0, 1]$ via min-max normalization. We simulate MCAR with a missing rate of 0.2 by removing each value independently according to a Bernoulli distribution. We also simulate an MAR scenario where the missing probability of the last 30% features depends on the values of the first 30% features³.

The initial imputation is performed by random sampling from the observed entries of each feature. All experiments are conducted using five-fold cross validation where the test set only goes through the re-imputation phase in each iteration.

Hyperparameters EMFlow is not sensitive to the choice of hyperparameters⁴. We use $\alpha = 10^6$ and choose $\rho_t = 0.99 \cdot t^{-0.8}$ as the step size schedule for all UCI datasets. During the training of EMFlow, the batch size is 256 and the learning rate is 1×10^{-4} .

Compared to MCAR, the initial imputation can be more difficult under MAR where the marginal observed density is distorted more. Therefore, the robust covariance estimation

³See the supplementary section for the details of how MAR is simulated.

⁴The insensitivity of EMFlow towards hyperparameters is presented in the supplementary section

in Eq. (15) is adopted by default under MAR. Specifically, we use $\beta = 10^{-2}$ for the first two iterations, $\beta = 10^{-3}$ for the next two iterations, and $\beta = 0$ for the remaining ones.

Results The imputation performance is evaluated by calculating the Root Mean Squared Error (RMSE) between the imputed and true values. As shown in Table 1, EMFlow performs constantly better than MCFflow under both MCAR and MAR settings for nearly all datasets. Additionally, We trained both models on the same machine with the same learning rate and batch size and plot how the training loss and RMSE on test set decrease over time in Figure 2. It shows that EMFlow converges at least 5 times faster than MCFflow. In fact, EMFlow converges within three iterations for most of the UCI datasets.

4.2. Image Datasets

We also evaluate EMFlow on MNIST and CIFAR-10. MNIST is a dataset of 28×28 grayscale images of handwritten digits [21], and CIFAR-10 is a dataset of 32×32 colorful images from 10 classes [19]. For both datasets, the pixel values of each image are scaled to $[0, 1]$. In this section, we simulate MCAR where each pixel is independently missing with various probabilities from 0.1 to 0.9.

The initial imputation is performed by nearest-neighbor sampling where a missing pixel is filled by one of its nearest neighbors. In our experiments, the standard 60,000/10,000 and 50,000/10,000 training-test set partitions are used for MNIST and CIFAR-10 respectively.

Hyperparameters For all experiments in this section, the step size schedule of online EM is again $\rho_t = 0.99 \cdot t^{-0.8}$. For MNIST and CIFAR-10, we choose α to be 5×10^8 and 1×10^6 respectively. Since image datasets have much larger dimensions than UCI datasets, the super-batch approach with a size of 3000 is adopted. Additionally, the robust covariance estimation used by UCI datasets is also applied to CIFAR-10.

Results Table 2 shows that EMFlow outperforms its competitor in most situations especially for CIFAR-10 in terms of RMSE. We also compare these two methods with respect to the accuracy of post-imputation classification. For this purpose, a LeNet-based model and a VGG19 model were trained on the original training sets of MNIST and CIFAR-10 respectively. These models then made predictions on the imputed test sets under different missing rates. Table 3 shows that EMFlow yields slightly better post-imputation prediction accuracy than MCFflow on MNIST, while the improvement is much more significant on CIFAR-10. Those findings are in good agreement with the results of imputation accuracy in Table 2.

5. Conclusion

We propose a novel architecture EMFlow for missing data imputation. It combines the strength of the online EM and the normalizing flow to learn the density estimation in the presence of incomplete data while performing imputation. Various experiments with multivariate and image datasets show that EMFlow significantly outperforms its state-of-art competitor with respect to imputation accuracy as well as the convergence speed under a wide range of missing rates and different missing mechanisms. The accuracy of post-imputation classification on image datasets also demonstrates the superior EMFlow’s ability of recovering semantic structure from incomplete data.

References

- [1] Vincent Audigier, François Husson, and Julie Josse. Multiple imputation for continuous variables using a bayesian principal component analysis. *Journal of statistical computation and simulation*, 86(11):2140–2156, 2016. 1
- [2] Marcelo Bertalmio, Guillermo Sapiro, Vincent Caselles, and Coloma Ballester. Image inpainting. In *Proceedings of the 27th annual conference on Computer graphics and interactive techniques*, pages 417–424, 2000. 1
- [3] AE Brockwell. Universal residuals: A multivariate transformation. *Statistics & probability letters*, 77(14):1473–1478, 2007. 2
- [4] Yuri Burda, Roger Grosse, and Ruslan Salakhutdinov. Importance weighted autoencoders. *arXiv preprint arXiv:1509.00519*, 2015. 2
- [5] S van Buuren and Karin Groothuis-Oudshoorn. mice: Multivariate imputation by chained equations in r. *Journal of statistical software*, pages 1–68, 2010. 1
- [6] Olivier Cappé and Eric Moulines. On-line expectation–maximization algorithm for latent data models. *Journal of the Royal Statistical Society: Series B (Statistical Methodology)*, 71(3):593–613, 2009. 1, 3, 9
- [7] Yilun Chen, Ami Wiesel, and Alfred O Hero. Robust shrinkage estimation of high-dimensional covariance matrices. *IEEE Transactions on Signal Processing*, 59(9):4097–4107, 2011. 5
- [8] Mark Collier, Alfredo Nazabal, and Christopher KI Williams. Vaes in the presence of missing data. *arXiv preprint arXiv:2006.05301*, 2020. 2
- [9] Dua Dheeru and E Karra Taniskidou. Uci machine learning repository. 2017. 5
- [10] Marco Di Zio, Ugo Guarnera, and Orietta Luzi. Imputation through finite gaussian mixture models. *Computational Statistics & Data Analysis*, 51(11):5305–5316, 2007. 1

Table 1. Imputation Results on UCI Datasets - RMSE (lower is better).

Data	MCAR		MAR	
	EMFlow	MCFlow	EMFlow	MCFlow
News	0.1394 ± 0.0007	0.1673 ± 0.0015	0.1715 ± 0.0004	0.1806 ± 0.0007
Air	0.0967 ± 0.0045	0.1106 ± 0.0037	0.0402 ± 0.0005	0.0545 ± 0.00010
Letter	0.1106 ± 0.0008	0.1207 ± 0.0002	0.1095 ± 0.0013	0.1273 ± 0.0012
Concrete	0.1467 ± 0.0040	0.2329 ± 0.0067	0.1333 ± 0.0062	0.1975 ± 0.0095
Review	0.2285 ± 0.0027	0.2344 ± 0.0036	0.1938 ± 0.0041	0.1909 ± 0.0043
Credit	0.1246 ± 0.0013	0.1347 ± 0.0018	0.0239 ± 0.0014	0.0276 ± 0.0015
Energy	0.0859 ± 0.0008	0.0923 ± 0.0011	0.1750 ± 0.0018	0.1760 ± 0.0020
CTG	0.1036 ± 0.0056	0.1403 ± 0.0047	0.1050 ± 0.0009	0.1529 ± 0.0028
Song	0.0253 ± 0.0001	0.0296 ± 0.0056	0.0241 ± 0.0002	0.0313 ± 0.0144
Wine	0.0757 ± 0.0013	0.0975 ± 0.0020	0.1020 ± 0.0018	0.1235 ± 0.0028

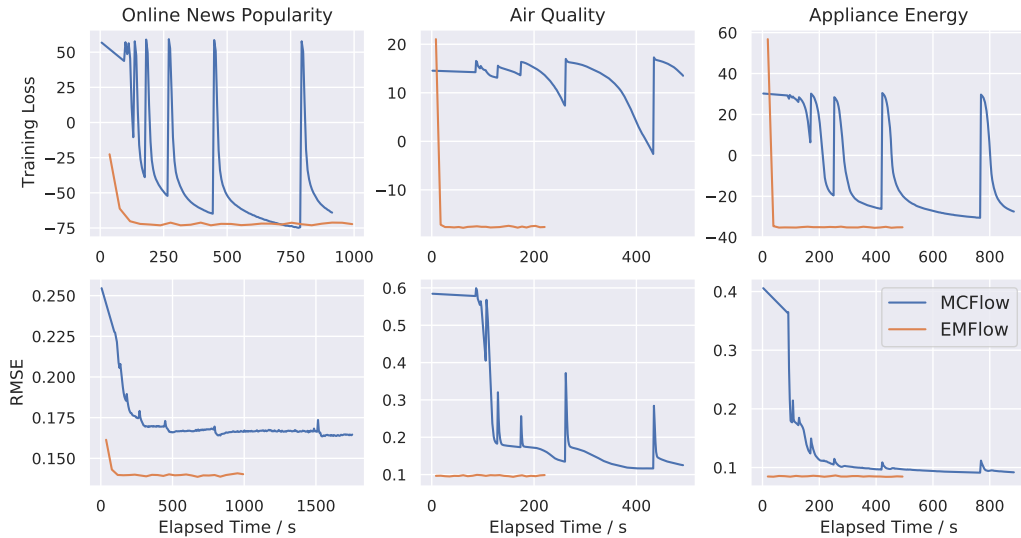


Figure 2. EMFlow architecture.

- [11] Laurent Dinh, David Krueger, and Yoshua Bengio. Nice: Non-linear independent components estimation. *arXiv preprint arXiv:1410.8516*, 2014. [1](#), [3](#)
- [12] Laurent Dinh, Jascha Sohl-Dickstein, and Samy Bengio. Density estimation using real nvp. *arXiv preprint arXiv:1605.08803*, 2016. [1](#), [3](#)
- [13] Jianqing Fan, Yingying Fan, and Jinchi Lv. High dimensional covariance matrix estimation using a factor model. *Journal of Econometrics*, 147(1):186–197, 2008. [5](#)
- [14] Pedro J García-Laencina, José-Luis Sancho-Gómez, and Aníbal R Figueiras-Vidal. Pattern classification with missing data: a review. *Neural Computing and Applications*, 19(2):263–282, 2010. [1](#)
- [15] Lovedeep Gondara and Ke Wang. Multiple imputa-
- tion using deep denoising autoencoders. *arXiv preprint arXiv:1705.02737*, 2017. [1](#)
- [16] Niels Bruun Ipsen, Pierre-Alexandre Mattei, and Jes Frellsen. not-miaw: Deep generative modelling with missing not at random data. *arXiv preprint arXiv:2006.12871*, 2020. [2](#)
- [17] Diederik P Kingma and Prafulla Dhariwal. Glow: Generative flow with invertible 1x1 convolutions. *arXiv preprint arXiv:1807.03039*, 2018. [1](#)
- [18] Diederik P Kingma and Max Welling. Auto-encoding variational bayes. *arXiv preprint arXiv:1312.6114*, 2013. [2](#)
- [19] Alex Krizhevsky, Geoffrey Hinton, et al. Learning multiple layers of features from tiny images. 2009. [6](#)
- [20] Ranjit Lall. How multiple imputation makes a difference. *Political Analysis*, 24(4):414–433, 2016. [1](#)

Table 2. Imputation Results on Image Datasets - RMSE (lower is better)

	Missing Rate	.1	.2	.3	.4	.5	.6	.7	.8	.9
MNIST	MCFlow	.0835	.0879	.0894	.0941	.1027	.1119	.1251	.1463	.2020
	EMFlow	.0726	.0775	.0832	.0901	.0986	.1100	.1260	.1504	.1951
CIFAR-10	MCFlow	.1083	.1112	.1179	.1273	.1340	.1387	.1466	.1552	.1702
	EMFlow	.0444	.0479	.0525	.0575	.0619	.0689	.0782	.0926	.1188

Table 3. Classification Accuracy on Imputed Image Datasets (higher is better)

	Missing Rate	.1	.2	.3	.4	.5	.6	.7	.8	.9
MNIST	MCFlow	.9894	.9878	.9878	.9871	.9840	.9806	.9659	.9331	.7732
	EMFlow	.9894	.9884	.9882	.9878	.9860	.9824	.9696	.9253	.7502
CIFAR-10	MCFlow	.8352	.7081	.5525	.4166	.3406	.2820	.2476	.2194	.1875
	EMFlow	.9085	.8974	.8783	.8535	.8116	.7446	.6214	.4868	.3127

[21] Yann LeCun, Léon Bottou, Yoshua Bengio, and Patrick Haffner. Gradient-based learning applied to document recognition. *Proceedings of the IEEE*, 86(11):2278–2324, 1998. [6](#)

[22] Steven Cheng-Xian Li, Bo Jiang, and Benjamin Marlin. Misgan: Learning from incomplete data with generative adversarial networks. *arXiv preprint arXiv:1902.09599*, 2019. [2](#)

[23] Roderick JA Little and Donald B Rubin. *Statistical analysis with missing data*, volume 793. John Wiley & Sons, 2019. [1, 2, 3](#)

[24] Chao Ma, Sebastian Tschiatschek, Konstantina Palla, José Miguel Hernández-Lobato, Sebastian Nowozin, and Cheng Zhang. Eddi: Efficient dynamic discovery of high-value information with partial vae. *arXiv preprint arXiv:1809.11142*, 2018. [2](#)

[25] Jinwen Ma, Lei Xu, and Michael I Jordan. Asymptotic convergence rate of the em algorithm for gaussian mixtures. *Neural Computation*, 12(12):2881–2907, 2000. [1](#)

[26] Pierre-Alexandre Mattei and Jes Frellsen. Miwae: Deep generative modelling and imputation of incomplete data sets. In *International Conference on Machine Learning*, pages 4413–4423. PMLR, 2019. [2](#)

[27] Xiao-Li Meng et al. On the rate of convergence of the ecm algorithm. *The Annals of Statistics*, 22(1):326–339, 1994. [1](#)

[28] Mehdi Mirza and Simon Osindero. Conditional generative adversarial nets. *arXiv preprint arXiv:1411.1784*, 2014. [2](#)

[29] Danilo Rezende and Shakir Mohamed. Variational inference with normalizing flows. In *International Conference on Machine Learning*, pages 1530–1538. PMLR, 2015. [1](#)

[30] Danilo Jimenez Rezende, Shakir Mohamed, and Daan Wierstra. Stochastic backpropagation and approximate inference in deep generative models. In *International conference on machine learning*, pages 1278–1286. PMLR, 2014. [1](#)

[31] Trevor W Richardson, Wencheng Wu, Lei Lin, Beilei Xu, and Edgar A Bernal. Mcflow: Monte carlo flow models for data imputation. In *Proceedings of the IEEE/CVF Conference on Computer Vision and Pattern Recognition*, pages 14205–14214, 2020. [2, 5](#)

[32] Badrul Sarwar, George Karypis, Joseph Konstan, and John Riedl. Item-based collaborative filtering recommendation algorithms. In *Proceedings of the 10th international conference on World Wide Web*, pages 285–295, 2001. [1](#)

[33] Peter Schmitt, Jonas Mandel, and Mickael Guedj. A comparison of six methods for missing data imputation. *Journal of Biometrics & Biostatistics*, 6(1):1, 2015. [1](#)

[34] RS Somasundaram and R Nedunchezhian. Evaluation of three simple imputation methods for enhancing preprocessing of data with missing values. *International Journal of Computer Applications*, 21(10):14–19, 2011. [1](#)

[35] Daniel J Stekhoven and Peter Bühlmann. Missforest—nonparametric missing value imputation for mixed-type data. *Bioinformatics*, 28(1):112–118, 2012. [1](#)

[36] Takeshi Teshima, Isao Ishikawa, Koichi Tojo, Kenta Oono, Masahiro Ikeda, and Masashi Sugiyama. Coupling-based invertible neural networks are universal diffeomorphism approximators. *arXiv preprint arXiv:2006.11469*, 2020. [3](#)

[37] CF Jeff Wu. On the convergence properties of the em algorithm. *The Annals of statistics*, pages 95–103, 1983. [1](#)

[38] Hai xian Wang, Quan bing Zhang, Bin Luo, and Sui Wei. Robust mixture modelling using multivariate t-distribution with missing information. *Pattern Recognition Letters*, 25(6):701–710, 2004. [1](#)

[39] Junyuan Xie, Linli Xu, and Enhong Chen. Image denoising and inpainting with deep neural networks. *Advances in neural information processing systems*, 25:341–349, 2012. [1](#)

[40] Raymond Yeh, Chen Chen, Teck Yian Lim, Mark Hasegawa-Johnson, and Minh N Do. Semantic image inpainting with perceptual and contextual losses. *arXiv preprint arXiv:1607.07539*, 2(3), 2016. 1

[41] Jinsung Yoon, James Jordon, and Mihaela Schaar. Gain: Missing data imputation using generative adversarial nets. In *International Conference on Machine Learning*, pages 5689–5698. PMLR, 2018. 2

[42] Ruofei Zhao, Yuanzhi Li, Yuekai Sun, et al. Statistical convergence of the em algorithm on gaussian mixture models. *Electronic Journal of Statistics*, 14(1):632–660, 2020. 1

6. Supplementary Material

6.1. Online EM for Missing Data imputation

In this section, the steps of vanilla EM in the context of missing data imputation are reviewed. We then show how the online EM framework proposed by Cappé and Moulines [6] can be easily applied here.

Given n i.i.d data points $\{\mathbf{z}_i = (\mathbf{z}_i^o, \mathbf{z}_i^m)\}_{i=1}^n$ distributed under $\mathcal{N}(\mu, \Sigma)$, the E-step of each EM iteration evaluates the conditional expectation of the complete data likelihood:

$$\begin{aligned} Q(\phi; \phi^{(t)}) &= \frac{1}{n} \sum_{i=1}^n Q_i(\phi; \hat{\phi}^{(t)}) \\ &= \frac{1}{n} \sum_{i=1}^n E_{\hat{\phi}^{(t)}} [\log \mathcal{N}(\mathbf{z}_i; \phi) | \mathbf{z}_i^o] \end{aligned} \quad (16)$$

where $\phi = (\mu, \Sigma)$, and $\hat{\phi}^{(t)} = (\hat{\mu}^{(t)}, \hat{\Sigma}^{(t)})$ are the estimates at the t^{th} iteration. We also follow the treatment by Cappé and Moulines [6] to normalize the conditional expectation by $1/n$ for easier transition to the online version of EM.

To calculate conditional expectation inside the summation, we can use the fact that the conditional distribution of \mathbf{z}_i^m given \mathbf{z}_i^o is still Gaussian:

$$\mathbf{z}_i^m | \mathbf{z}_i^o; \hat{\phi}^{(t)} \sim \mathcal{N}(\tilde{\mu}_i^{(t)}, \tilde{\Sigma}_i^{(t)}) \quad (17)$$

where

$$\begin{aligned} \tilde{\mu}_i^{(t)} &= \hat{\mu}_{\mathbf{m}_i}^{(t)} + \hat{\Sigma}_{\mathbf{m}_i \mathbf{o}_i}^{(t)} \left(\hat{\Sigma}_{\mathbf{o}_i \mathbf{o}_i}^{(t)} \right)^{-1} \left(\mathbf{z}_i^o - \hat{\mu}_{\mathbf{o}_i}^{(t)} \right), \\ \tilde{\Sigma}_i^{(t)} &= \hat{\Sigma}_{\mathbf{m}_i \mathbf{m}_i}^{(t)} - \hat{\Sigma}_{\mathbf{m}_i \mathbf{o}_i}^{(t)} \left(\hat{\Sigma}_{\mathbf{o}_i \mathbf{o}_i}^{(t)} \right)^{-1} \hat{\Sigma}_{\mathbf{o}_i \mathbf{m}_i}^{(t)}, \end{aligned} \quad (18)$$

\mathbf{m}_i and \mathbf{o}_i are the missing and observed masks respectively, and the subscripts of $(\hat{\mu}^{(t)}, \hat{\Sigma}^{(t)})$ represent the slicing indexes.

Then it's easily easy to find

$$\begin{aligned} Q_i(\phi; \hat{\phi}^{(t)}) &= -\frac{1}{2} \left[\left(\hat{\mathbf{z}}_i^{(t)} - \mu \right)^T \Sigma^{-1} \left(\hat{\mathbf{z}}_i^{(t)} - \mu \right) \right. \\ &\quad \left. + \text{Tr} \left(\left[\left(\Sigma^{-1} \right)_{\mathbf{m}_i \mathbf{m}_i} \right] \tilde{\Sigma}_i^{(t)} \right) \right] - \frac{1}{2} \log |2\pi\Sigma| \end{aligned} \quad (19)$$

where $\text{Tr}(\cdot)$ denotes the matrix trace, and $\hat{\mathbf{z}}_i^{(t)}$ is in fact the imputed data vector whose missing part is replaced by the conditional mean $\tilde{\mu}_i^{(t)}$.

When it comes to the M-step, the derivatives of $Q(\phi; \phi^{(t)})$ are calculated as

$$\begin{aligned} \frac{\partial Q}{\partial \mu} &= \frac{1}{n} \Sigma^{-1} \sum_{i=1}^n \left(\hat{\mathbf{z}}_i^{(t)} - \mu \right) \\ \frac{\partial Q}{\partial \Sigma^{-1}} &= -\frac{1}{2n} \sum_{i=1}^n \left(\hat{\mathbf{z}}_i^{(t)} - \mu \right) \left(\hat{\mathbf{z}}_i^{(t)} - \mu \right)^T \\ &\quad + \frac{1}{2} \left[\Sigma - \frac{1}{n} \sum_{i=1}^n \tilde{\Sigma}_i^{(t)} \right] \end{aligned} \quad (20)$$

where $\tilde{\Sigma}_i^{(t)}$ is $p \times p$ matrix satisfying $\tilde{\Sigma}_{i, \mathbf{m}_i \mathbf{m}_i}^{(t)} = \tilde{\Sigma}_i^{(t)}$ and all other elements equal to 0.

Therefore, the maximizer of $Q(\phi; \hat{\phi}^{(t)})$ are

$$\begin{aligned} \hat{\mu}^{(t+1)} &= \frac{1}{n} \sum_{i=1}^n \hat{\mathbf{z}}_i^{(t)}, \\ \hat{\Sigma}^{(t+1)} &= \frac{1}{n} \sum_{i=1}^n \left[\left(\hat{\mathbf{z}}_i^{(t)} - \mu^{(t+1)} \right) \left(\hat{\mathbf{z}}_i^{(t)} - \mu^{(t+1)} \right)^T + \tilde{\Sigma}_i^{(t)} \right]. \end{aligned} \quad (21)$$

It's clear that the EM algorithm needs the process the whole dataset at each iteration, which becomes impractical when dealing with huge datasets. To address this problem, Cappé and Moulines [6] propose to replace the reestimation functional in the E-step by a stochastic approximation step:

$$\begin{aligned} \hat{Q}^{(t+1)}(\phi) &= (1 - \rho_{t+1}) \hat{Q}^{(t)}(\phi) \\ &\quad + \rho_{t+1} \cdot \frac{1}{|B|} \sum_{i \in B} E_{\hat{\phi}^{(t)}} [\log f(\mathbf{z}_i; \psi) | \mathbf{z}_i^o] \end{aligned} \quad (22)$$

where f is the probability density of complete data, $B \subset \{1, \dots, n\}$ denotes the indexes of a mini-batch of samples, and $|B|$ is the batch size.

Under some mild regulations such as the complete data model belongs to exponential family [6], Eq. (22) boils down to a stochastic approximation of the estimates of sufficient statistics:

$$\hat{s}^{(t+1)} = (1 - \rho_{t+1}) \hat{s}^{(t)} + \rho_{t+1} \frac{1}{|B|} \sum_{i \in B} E_{\hat{\phi}^{(t)}} [S(\mathbf{z}) | \mathbf{z}_i^o] \quad (23)$$

where $S(\mathbf{z})$ is the sufficient statistic of f .

Note that the sufficient statistics for multivariate Gaussian are just sample mean and sample covariance. Therefore, Eq. (7) follows immediately from (23).

6.2. Affine Coupling Layers

The building block of RealNVP is the affine coupling layer $f_{\text{aff}} : \mathbf{x} \mapsto \mathbf{y}$ defined as

$$\begin{aligned} \mathbf{y}_{1:d} &= \mathbf{x}_{1:d} \\ \mathbf{y}_{d+1:p} &= \mathbf{x}_{d+1:p} \odot \exp(s(\mathbf{x}_{1:d})) + t(\mathbf{x}_{1:d}) \end{aligned} \quad (24)$$

where the scale and shift parameters $s(\cdot)$ and $t(\cdot)$ are usually implemented by neural networks, and \odot is the element-wise product.

Therefore, the input \mathbf{x} are split into two parts: the first d dimensions stay the same, while the other dimensions undergo an affine transformation whose parameters are the functions of the first d dimensions.

The building block of RealNVP is the affine coupling layer $f_{\text{aff}} : \mathbf{x} \mapsto \mathbf{y}$ defined as

$$\begin{aligned} \mathbf{y}_{1:d} &= \mathbf{x}_{1:d} \\ \mathbf{y}_{d+1:p} &= \mathbf{x}_{d+1:p} \odot \exp(s(\mathbf{x}_{1:d})) + t(\mathbf{x}_{1:d}) \end{aligned} \quad (25)$$

where the scale and shift parameters $s(\cdot)$ and $t(\cdot)$ are usually implemented by neural networks, and \odot is the element-wise product.

Therefore, the input \mathbf{x} are split into two parts: the first d dimensions stay the same, while the other dimensions undergo an affine transformation whose parameters are the functions of the first d dimensions.

6.3. Simulate MAR on UCI Datasets

To simulate MAR, the first 70% features of each data point \mathbf{x}_i is retained, and the remaining 30% features are removed with probability:

$$\text{sigmoid} \left(\sum_{j=1}^{\lfloor 0.7D \rfloor} x_{ij} \right) \quad (26)$$

where $\lfloor \cdot \rfloor$ denotes the integer part of a number.

Note that different data sets would exhibit different missing rates under our MAR setting. Table shows the dimensions of UCI data sets used in our experiment as well as their MAR missing rates for the last 30% features.

6.4. Robustness to Hyperparameters

There are two most important two hyperparameters specific to EMFlow. One is the power index γ in the step size schedule of online EM (see Eq. (9)), while the other is the

Table 4. Information of UCI data sets.

Data	Features	Samples	MAR missing rate
News	60	39644	0.35
Air	13	9357	0.62
Letter	16	19999	0.57
Concrete	9	1030	0.50
Review	24	5454	0.49
Credit	23	30000	0.30
Energy	28	19735	0.39
Crop	21	2126	0.29
Song	90	92743	0.32
Wine	12	6497	0.26

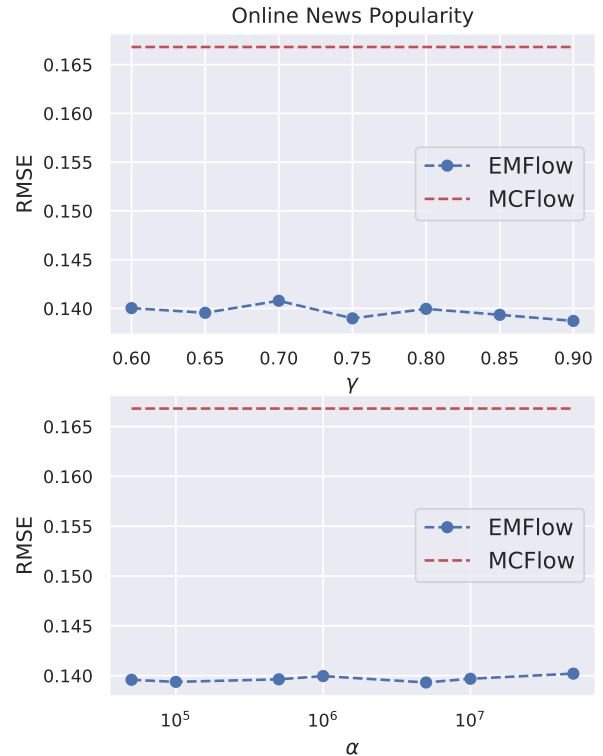


Figure 3. EMFlow architecture.

strength of the reconstruction error α in the objective (see Eq. (13)). From our extensive experiments, $\gamma \in [0.6, 0.9]$ often leads to consistent results. On the other hand, a practical guide for choosing α is to make the magnitudes of first and second term of Eq. (13) don't differ too much.

Figure 3 shows RMSE on the test set of Online News Popularity dataset versus different values of γ and α , while all other hyperparameters are kept fixed. The RMSEs in all configurations are well below that obtained by MCFlow, and its fluctuation is almost negligible.